A strategy for prediction of the elastic properties of epoxy-cellulose nanocrystal-reinforced fiber networks

Johnathan E. Goodsell, Robert J. Moon, Alionso Huizar, and R. Byron Pipes

KEYWORDS: Laminate theory, Multi-scale modeling, Elasticity, Network composites, Cellulose nanocrystals

SUMMARY: The reinforcement potential of cellulose nanocrystal (CNC) additions on an idealized 2-dirmensional (2-D) fiber network structure consisting of micron sized fiber elements was investigated. The reinforcement mechanism considered in this study was through the stiffening of the micron sized fiber elements via a CNC-epoxy coating. A hierarchical analytical modeling approach was used to estimate the elastic properties spanning three different structural features; i) micromechanics for CNC-epoxy properties, ii) laminate theory for fiber elements coated with CNC-epoxy, and iii) a 2-D network model for an assembly of interconnected fiber elements. The extent to which CNC-epoxy coating can stiffen a fiber element was dependent on the CNC volume fraction, CNC-epoxy layer thickness, CNC alignment, CNC aspect ratio, and the original stiffness of the fiber element. Calculations suggest there is a potential for CNC additions to stiffen network structures, the extent to which is strongly depending on the initial fiber element stiffness. Incorporation of limited experimental observations into the model and fiber element properties typical of fibers used in paper products, however, suggests that the enhancement of CNCs on a wood fiber element and thus on the network structure, may be limited.

ADDRESSES OF THE AUTHORS: Johnathan E. Goodsell (jgoodsel@purdue.edu) **Alionso Huizar, R. Byron Pipes** (bpipes@purdue.edu) Purdue University, 701 West Stadium Ave, West Lafayette, IN 47907; **Robert J. Moon** (robertmoon@fs.fed.us), US Forest Service, Forest Products Laboratory, Madison, Wisconsin 53726.

Cellulose nanomaterials are cellulose based particles, having at least one dimension in the nanoscale, extracted from various plant materials, algae, bacteria and marine animals (tunicates). The resulting nanoparticle morphology, properties, and characteristics are dependent on the cellulose source and the extraction process. Two types of nanoparticles extracted from trees and plants are cellulose nanocrystals (CNCs, ~3-5 nm wide, ~50-500 nm in length) and cellulose nanofibrils (CNF, ~5-50 nm wide, 500 nm to microns in length). Here, we use the term cellulose nanomaterial (CNM) to broadly refer to all cellulose based nanoparticles. In general, CNMs have several characteristics that make them desirable as reinforcement phase, such as, relatively high aspect ratio, nano size-scale fibril morphology, favorable mechanical properties, low density, low coefficient of thermal expansion, and surfaces accessible to chemical functionalization, to name a few (Moon et al. 2011; Samir et al. 2005; Siro, Plackett 2010). As a result of these material characteristics, CNMs have been used in the development of various composite materials and structures, such as films, foams, continuous fiber, microcapsules, network structures, etc. They have been incorporated into many polymer systems as a reinforcement phase (Samir et al. 2005; Siro, Plackett 2010), and used to produce CNM films with nano size scale network structures that have high stiffness and strength (Moon et al. 2011; Reising et al. 2012).

CNMs have also been used for modifying the properties of individual natural fibers (Juntaro et al. 2008; Pommet et al. 2008) and micron size scale network structures, such as paper (Hassan et al. 2011; Joseleau et al. 2012; Lavoine et al. 2012; Ma et al. 2011; Sehaqui et al. 2013). CNMs can been added to network structures in several ways, such as; i) casting an aqueous suspension of CNM on to the surface of a preformed cellulose fiber network structure (Aulin et al. 2010; Lavoine et al. 2012; Ma et al. 2011; Syverud, Stenius 2009), ii) co-mixing CNM materials with the micron sized pulp particles, (Hassan et al. 2011; Joseleau et al. 2012; Sehaqui et al. 2013) and iii) use CNM-polymer emulsions to penetrate preformed network structure and coat individual fibers and the fiber-fiber joints (Huang et al. 2012). The majority of the studies investigating CNM additions to a preformed network structure have been with CNFs or bacterial cellulose (BC) materials. The addition of CNF materials to non-woven fiber network structures has primarily focused on improving barrier properties (e.g. moisture, oxygen permeability) (Aulin et al. 2010; Lavoine et al. 2012; Ma et al. 2011; Syverud, Stenius 2009). The mechanical properties of the nonwoven networks have also been shown to be modified (Hassan et al. 2011; Joseleau et al. 2012; Sehaqui et al. 2013), in which the addition of CNF via co-mixing with pulp fibers was shown to increase tensile strengths. The study by Sehaqui et al., showed that 10 vol% CNF additions resulting in an ~60% increase in the tensile strength index, this increase was attributed to the increase in density of the network structure (i.e. lower porosity, and thus increased volume fraction of load bearing material).

To the authors' knowledge, there have been no modeling studies investigating the reinforcing potential of CNM additions to a preformed network structure consisting of micron sized fiber elements. In contrast, the reinforcement effect/potential of CNMs in polymer matrix composites have been investigated via various micromechanical models, typically using mean field (Halpin-Tsai, Halpin-Kardos, etc.) and percolation (connected CNM network within the matrix) approaches, as previously reviewed (Moon et al. 2011; Samir et al. 2005). Likewise, various network/lattice modeling approaches have been used to assess or predict the properties of fiber network systems (applicable to wood fibers, spun fibers, and CNMs), in particular, the elastic (Astrom et al. 1994; Bronkhorst 2003; Liu et al. 2010;

Silberstein et al. 2012; Wu, Dzenis 2005), plastic (Bronkhorst 2003; Silberstein et al. 2012), and fracture properties (Liu et al. 2010). The network structures of paper and CNM films are inherently complicated and difficult to duplicate in network models, because of this there will always be some discrepancy in the properties predicted from models and what is experimentally measured. Nonetheless, these approaches have provided insight as to the role of various parameters on the effective network properties, such as, fiber orientation, fiber stiffness, network interconnectivity, network density, fiber-fiber joint properties, 2-dimensional (2D) verses 3-dimentional (3D) configurations, etc. However, to date these network models have not been applied to assess the effect of nanoparticle additions to network properties. It is yet unclear as how to model the reinforcing potential of CNMs to such network structures.

The motivation of this study was to provide an "upper bound" when it comes to mechanical property enhancement of network structures, consisting of micron sized fiber elements, by the addition of CNCs. The relatively high mechanical properties of CNCs make it tempting to believe that only small amounts (e.g. 1-2 vol%) need to be added to a network structure to vastly increase the network properties. Two fundamental questions to be answered are: 1) What is the critical vol% CNC additions necessary to affect the macroscopic network properties? 2) What is the potential maximum reinforcement potential of CNC additions? With this in mind, an idealized model system was conceived, not to duplicate the structure of paper, but rather to have a simple platform from which it is possible to address these questions.

A simple modeling approach was developed to estimate the reinforcement potential of CNCs (i.e. nano-sized particles) additions to network structures consisting of micron sized fiber elements. The modeling approach used an idealized 2-D network structure for simulating the elastic properties (elastic modulus and Poison's ratio) of a micron size scale fiber network structure. The modification to the network elastic properties could occur via changes in stiffness of either the fiber element and/or the joint between overlapping fibers elements. Considered in this study was for the special case where CNC additions occurred through CNC-epoxy coating that preferentially bonded to the fiber elements, reinforcing them, which then subsequently reinforces the overall network structure. A micromechanical model was used to estimate the elastic properties of the CNC-epoxy coating, while laminate theory was used to estimate the elastic properties of an individual fiber element coated with CNC-epoxy. By considering both the micromechanical and laminate models together, an estimate of the achievable stiffening imparted by the CNC-epoxy coating on the individual fiber elements could be calculated. The elastic modulus of the CNC-epoxy coated fiber element was then used as an input parameter for the idealized 2-D network model and the subsequent network elastic modulus and poison's ratio were calculated

The focus of this preliminary study was to assess the extent to which CNC additions could alter the elastic properties (elastic modulus and Poison's ratio) of a network structure consisting of micron sized fiber elements. The CNC addition occurred through a CNC-epoxy coating on individual fiber elements, reinforcing them, and thus altering the elastic properties of the network. The role of CNC volume fraction, aspect ratio, alignment, CNC-epoxy coating thickness, the network joint stiffness, and the fiber element stiffness on the elastic properties of the idealized 2-D network were also assessed. Though not directly related to paper, some insight may be gained.

Materials and Methods

Fiber element and CNC geometry

The fiber element used had a width (W_f), thickness (t_f), and length (L_f) of 30 μm, 10 μm, and 180 μm, respectively. The elastic modulus of the fiber element in the fiber direction, E_f, was either 15 GPa or 25 GPa, which are within the range of 5-27 GPa reported in the literature for southern yellow pine fibers (Mott et al. 2002). The CNC particles were considered to be rod-like having an aspect ratio, S_{CNC}, of either 20 or 100, which are toward the upper range of reported values of ~5 to 70 for CNCs extracted from wood and plant materials (Araki et al. 1998; Bai et al. 2009; Beck-Candanedo et al. 2005; Bondeson et al. 2006; Habibi et al. 2010). Note that with the micromechanical model used in this study, only the CNC aspect ratio is needed. The elastic moduli in the CNC longitudinal axis, E_{CNC} = 150 GPa, was used, which was within the range reported (105-220 GPa) based on experimental measurements on CNM materials (Eichhorn 2011; Iwamoto et al. 2009; Rusli, Eichhorn 2008; Sturcova et al. 2005) and model predictions of cellulose Iβ (Dri et al. 2013; Eichhorn 2011; Moon et al. 2011). A value E_{CNC}=150 GPa should be considered an upper bound estimate for CNCs extrated from wood/plant cellulose sources, and we have used this here so that we can assess the upper limit of the CNC reinforcement potential.

Hierarchical model development

A hierarchical modeling approach was used to investigate the elastic properties of an idealized 2-D network structure, in which the micron sized fiber elements making up the network, were reinforced by the addition of CNC-epoxy coating. The approach utilizes several conventional composites modeling approaches to span the length scales and to develop effective continuum properties of the reinforced network (see *Fig 1*). Three modeling techniques were used: i) micromechanics to estimate CNC-epoxy properties (i.e. the nano length scale), ii) laminate theory to estimate the properties of individual fiber elements coated with CNC-epoxy (i.e. the micro length scale), and iii) the idealized 2-D network model to estimate the properties of an assembly of interconnected fibers (i.e. macro length scale). Each modeling component is done separately. Micro-mechanics allows determination of the effective elastic properties of the CNC-epoxy composite, which are used as the input values within the laminate theory calculations for the CNC-epoxy layer coating the fiber element. Laminate theory provided a model to estimate the elastic

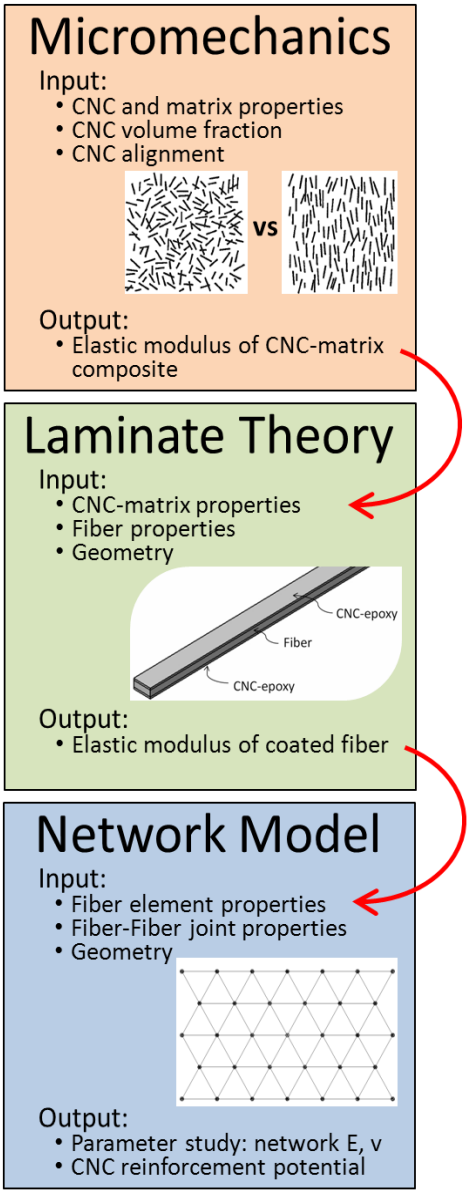

Fig 1 - Diagram flow of the hierarchical analytical model approach used in this study to investigate the contribution of CNC reinforcement over various length scales.

properties of the CNC-epoxy coated fiber element, which are used as input for the fiber element properties within the 2-D network model. Finally, effective properties of the isotropic network were then determined by the finite-element method with the element properties determined in the prior two steps.

The idealized 2-D network model was chosen for simplicity and provides insight into the properties for arrays of this geometry. Despite its simplicity, this model allows the ability to investigate the changes in network properties as a result of modification in the fiber element properties by the CNC additions. Additionally the inclusion of both the micromechanical and laminate models allow CNC parametric-property assessment to be completed and thus identify achievable stiffening imparted by the CNC on the network. For the parametric study (CNC alignment, volume fraction, aspect ratio, CNC-epoxy coating thickness, the network joint stiffness, and the fiber element stiffness), the values used for each parameter were intentionally chosen to be extremes, with the desire to identify potential upper and lower bounds. For example: the two extremes for the CNC alignment, was collimated versus random, where as in a "real" system the degree of CNC alignment would likely fall somewhere in-between these. Additionally, many other assumptions used in the study, from material properties, to interfaces properties in the micromechanical and laminate theory models where chosen to maximize properties. For example, E_{CNC}=150 GPa and S_{CNC}=100 are upper estimates. The upper bound of an idealized network system was intentionally investigated with the understanding that the performance of 'real' network systems will fall below this bound, the implications of which are discussed. Note that for each model the specific assumptions used will be listed in their corresponding section.

Micromechanics for CNC-epoxy composite

Micromechanics was used to estimate the elastic properties of a CNC-epoxy material that would subsequently coat the fiber elements making up the network structure. It was assumed that CNC additions to epoxy acted as expected for conventional composites, in which there were no "nano effects" (i.e. nanoscale phenomena) altering the properties of the epoxy or the CNC-epoxy interface, etc.. Parameter-property relationships for CNC-epoxy composites are needed to help guide the configuration of the composite coatings such that it has sufficient stiffness to enhance the elastic properties of the fiber element. The effective elastic properties were estimated using Halpin-Tsai (Halpin, Kardos 1976) equations for discontinuous CNC with an assumed aligned CNC configuration, a fixed CNC aspect ratio, S_{CNC}, and perfect interface between CNC and epoxy. The effective Young's modulus of CNC-epoxy composite measured in a direction parallel to the CNC alignment, E_{ca}, was calculated by:

$$E_{ca} = E_e \frac{E_{CNC}(1+2S_{CNC}V_{CNC})+2S_{CNC}E_eV_e}{E_{CNC}V_e+E_e(2S_{CNC}+V_{CNC})} \quad [1]$$

where E_{CNC}, E_e, V_{CNC}, and $V_e = 1\text{-}V_{CNC}$ are the Young's modulus, and volume fraction of CNC or epoxy, respectively. The reinforcement efficiency of randomly oriented CNC is expected to be lower than the highly aligned configuration. The elastic modulus for CNCs in a 2-D random array within the epoxy, E_{cr}, was taken to be equal to one-third the collimated CNC system (i.e. E_{cr} = 1/3 E_{ca}), following the laminate approximation first suggested by Halpin and Pagano (Halpin, Pagano 1969; Halpin et al. 1971). Calculations were completed using E_e = 3.8 GPa and E_{CNC} = 150 GPa. Variations of V_{CNC} (from 0 to 1) and S_{CNC} (20 and 100) on E_{ca} and E_{cr} were investigated. The role of the CNC orientation state was assessed by comparing E_{ca} to E_{cr} (i.e. aligned versus random).

Laminate theory for CNC-epoxy coated fiber element

The laminate composite geometry has a central core consisting of the fiber element with a coating of CNC-epoxy on the upper and lower surfaces (*Fig 2*). It was

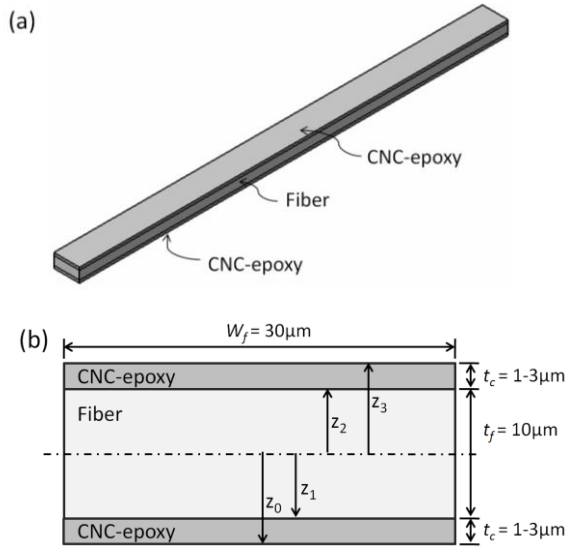

Fig 2 - Schematic of fiber CNC-epoxy laminated fiber element model. a) reinforced fiber element geometry, and b) cross-section of reinforced fiber element.

assumed that the interfaces between the CNC-epoxy layers and the fiber element core were perfect. While differences in this laminate cross-sectional geometry affect bending stiffness, it has little effect upon the extensional stiffness of the fiber for extensional elements in the network model. The extensional stiffness properties of the CNC-epoxy coated fiber element can be calculated from the laminate stiffness matrix: A_{ij}. The stiffness matrix is defined in terms of the elastic properties of the layers, Q_{ij}, and the distance of the top and bottom of each layer from the mid-plane, z_k and z_{k-1}, respectively, as shown in *Eq 2*.

$$A_{ij}=\sum_{k=1}^{N} Q_{ij}(z_k - z_{k-1}) \qquad [2]$$

For both the fiber and the CNC-epoxy layer the elastic property matrix is

$$Q_{ij}=\begin{bmatrix} Q_{11} & Q_{12} & 0 \\ Q_{12} & Q_{22} & 0 \\ 0 & 0 & Q_{66} \end{bmatrix} \qquad [3]$$

where,

$$Q_{11}= Q_{22}= \frac{E_x}{(1-\nu_x{}^2)}, \quad Q_{12}= \frac{\nu_x E_x}{(1-\nu_x{}^2)}, \quad Q_{66}= \frac{E_x}{2(1+\nu_x)} \qquad [4]$$

For the fiber layer, the values for $E_x = E_f$ and $\nu_x = \nu_f$ are used. For the CNC-epoxy layer with random CNC orientation, by assuming that ν_{cr} is the same as that for the epoxy, ν_e= 0.36, then *Eq 4* can be used to define the Q_{ij} terms, with $E_x = E_{cr}$, and $\nu_x = \nu_e$. While for the case of CNC-epoxy with aligned CNCs, the stiffness terms are given as:

$$Q_{11}= \frac{E_{ca}}{\left(1-\nu_e{}^2\frac{E_e}{E_{ca}}\right)}, \quad Q_{22}= \frac{E_e}{\left(1-\nu_e{}^2\frac{E_e}{E_{ca}}\right)}$$

$$Q_{12}= \frac{\nu_e E_e}{\left(1-\nu_e{}^2\frac{E_e}{E_{ca}}\right)}, \quad Q_{66}=G_e \qquad [5]$$

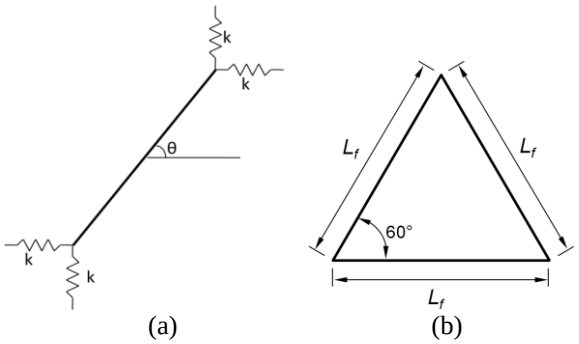

Fig 3 - Network structure, a) fiber element with elastic modulus of E_f, and spring constants, k, and b) representative volume element consisting of a network of 3 fiber elements of length L_f, interesting at θ=60°.

where G_e is the shear modulus of the epoxy (1.88 GPa). Given the A_{ij}, the effective modulus of the laminated composite, E_{lx}, can be calculated by,

$$E_{lx}=\frac{A_{11}A_{22}-A_{12}{}^2}{A_{22}h} \qquad [6]$$

where h is the total thickness of the laminate composite (i.e. the fiber layer plus the two CNC-epoxy layers). For either the random or aligned CNC orientation within the CNC-epoxy layers, E_{lr}, and E_{la}, respectively, can be calculated using the corresponding inputs for A_{11}, A_{22} and A_{12}. Laminate composite propeties were cacluated for cases of: E_f= 15 and 25 GPa, CNC-epoxy thickness of t_c= 1 and 3 µm, S_{CNC} = 20 and 100, and for random verse allinged CNC configuration.

Network model

A 2-D network model was constructed as an array of fiber extensional elements. Each fiber element, shown in *Fig 3a*, was modeled with ten linear beam finite elements along its length, L_f. Each fiber element was attached at the cross-over points by two orthogonal linear springs of equal spring constant, k (N/m). An isotropic network is accomplished by specifying a unit-cell geometry (*Fig 3b*) where the fiber elements in the network form an equilateral triangle, representing an array of fiber elements oriented at 0/±60 degrees. As such, the effective mechanical properties of the network will be isotropic. The Abaqus finite-element code was used to construct the fiber network unit cell (RVE with 3 fiber elements) and network geometries studied having 76 fiber elements (*Fig 4*). This network geometry was a single fiber in thickness, t_f, and only the planar properties of the network were examined.

The network elastic modulus, E_{net}, and Poisson's ratio, ν_{net}, were calculated for neat fiber networks and fiber networks in which the individual fibers were coated with the CNC-epoxy composite. Calculation of these elastic parameters was completed by applying a state of uniaxial stress to the network through horizontal nodal forces at the one lateral extremity, while fixing the axial displacement at the opposite end of the network (*Fig 4a*). The boundary layer phenomenon at the loading boundaries, associated with St. Venant's principle

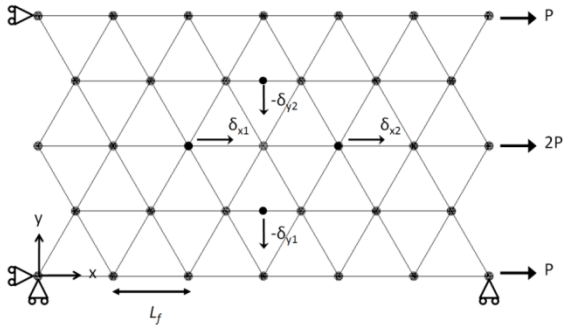

(a)

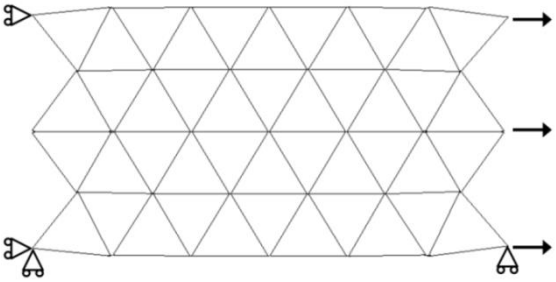

(b)

Fig 4 - Network structure model consisting of 76 fiber elements for axial extension, a) boundary conditions, showing the location of the nodal displacements, δ_x and δ_y, used for property calculations, and b) deformation shape for axial extension in loading direction showing minimal edge effects for the central regions used for property calculations.

(Timoshenko, Goodier 1951), dampen out within one element length so that deformations measured at the interior of the network can be considered to be independent of the boundary induced disturbances due to point nodal loads. Nodal displacements were used to determine the average axial stress, σ_x, axial strain, ε_x, and transverse strain ε_y:

$$\sigma_x = \frac{P}{L_f\, t_f \sin 60}, \quad \varepsilon_x = \frac{\delta_{x2} - \delta_{x1}}{2L_f}, \quad \varepsilon_y = \frac{\delta_{y2} - \delta_{y1}}{2L_f \sin 60} \qquad [7]$$

from which $E_{net} = \sigma_x/\varepsilon_x$ and $\nu_{net} = \varepsilon_y/\varepsilon_x$ could be calculated:

$$E_{net} = \frac{2P}{(\delta_{x2} - \delta_{x1}) t_f \sin 60}$$

$$\nu_{net} = \frac{\delta_{y2} - \delta_{y1}}{(\delta_{x2} - \delta_{x1}) \sin 60} \qquad [8]$$

The density of the fiber network model can be adjusted by altering the fiber element length between cross-over points, L_f. The effective density of the neat fiber network, ρ_{net}, can be expressed in terms of the density of the fiber element, ρ_f, the effective fiber volume fraction within the network (V_{net}), and the ratio of the fiber cross-sectional width to the distance between cross-over points (W_f/L_f):

$$\rho_{net} = \rho_f V_{net} = \rho_f \left[2\sqrt{3} \left(\frac{W_f}{L_f} \right) - 3 \left(\frac{W_f}{L_f} \right)^2 \right] t_f \qquad [9]$$

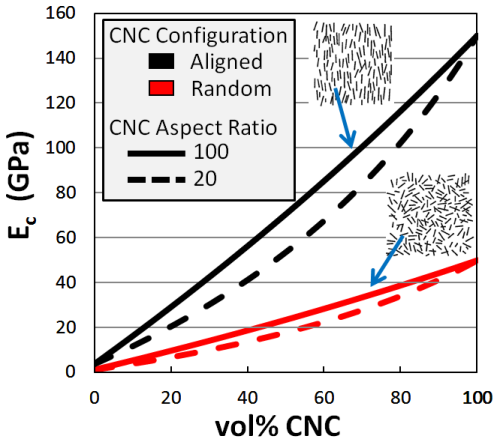

Fig 5 - Effective elastic modulus, E_c, of CNC-epoxy matrix composites as a function of: CNC volume percent, CNC configuration (random and aligned), and CNC aspect ratio, S_{CNC}.

The fiber element used in this study (with ρ_f= 1.5 g/cm^3, W_f = 30 µm, t_f=10 µm, L_f = 180 µm) resulted in a network density of ρ_{net} = 0.78 g/cm^3.Refrence to equation in text, *Eq 1*.

Results and Discussions

CNC reinforcement of epoxy

The results of the Halpin-Tsai calculations are shown in *Fig 5*, which summarizes the influence of CNC aspect ratio (20 vs. 100), CNC vol% (0-100), and CNC orientation (random vs. aligned) on E_c of CNC-epoxy composite. For the aligned CNC configuration, the properties were measured in the direction parallel to the CNC alignment. As expected, E_c increased for increasing CNC vol%, CNC alignment, and S_{CNC} increases E_c, in which increases in E_c appear to be more sensitive to CNC alignment than to S_{CNC}.

Comparison of these predictions to experimentally measured properties of CNC-epoxy shows some reasonable agreement for 0-24 vol% CNC additions (Tang, Weder 2010; Xu et al. 2013). The study by Tang and Weder produced CNC-epoxy composites films (in plane random CNC configuration) and investigated the reinforcement potential for CNCs from two different sources; CNCs extracted from cotton (aspect ratio less than 10), and from tunicate (aspect ratio ~85). The effective composites elastic modulus increased from 1.6 GPa of the neat epoxy, to a maximum at 24 vol% CNC-epoxy of ~ 3.6 GPa, and 4.7 GPa, for the cotton and tunicate CNC respectively. After adjusting for the differences in the elastic modulus for the neat epoxy, the model only modestly over predicts the experimentally measured composite elastic modulus, but more importantly shows similar trends (i.e. increase in elastic modulus for higher CNC aspect ratio, and CNC vol%). Further, the increased CNC aspect ratio in the model relative to Tang and Weder's experiments may also account for the greater reinforcement predicted by the model. We could not find any studies that incorporate more than 24 vol% CNCs into epoxy, but there has been

work with neat CNC films (i.e. 100 vol% CNC, not functionalized). The study by Reising et al. (Reising et al. 2012) investigated the role of CNC alignment on the mechanical properties of neat CNC films. The measured elastic modulus of 15 GPa (random), and 30 GPa (highly aligned), were much lower than the predicted values (at 100 vol% CNC in *Fig 5*) of 50 GPa, and 150 GPa, respectively. This overestimate in model predictions can partially be attributed to our use of E_{CNC}=150 GPa, and the assumption of perfect CNC-epoxy interface. Thus, the model over estimates the composite elastic modulus, the extent of this is small (~10-20%) at the lower vol% CNC, but is very large (>300%) at the 100 vol% CNC concentration.

The implications of this is that the output from this modeling component are upper bound elastic properties estimates, and will affect the prediction of the laminate theory model, and thus subsequently the property estimates from the 2-D network model.

CNC-epoxy reinforcement of fiber element

The effective elastic modulus of the CNC-epoxy coated fiber element laminate system (E_{lx}), is shown in *Fig 6* for both the random (E_{lr}) and aligned (E_{la}) CNC configuration. The resulting E_{lx} is a function of the CNC alignment, CNC-epoxy coating thickness, CNC aspect ratio, vol% CNC, and by E_f. The CNC alignment was the dominant factor influencing reinforcement, followed by CNC-epoxy coating thickness, and then aspect ratio.

To increase the elastic modulus of the fiber element it is necessary for the CNC-epoxy coating to have a higher elastic modulus than the fiber element (i.e. $E_c > E_f$). A unique critical condition occurs for each sample configuration (e.g., CNC-epoxy coating thickness, CNC alignment, S_{CNC}, vol% CNC, and E_f) and can be seen in *Fig 6* where the plots cross over at E_f = 15 or 25 GPa. As expected, fiber elements with greater E_f will be more difficult to reinforce, requiring higher CNC-epoxy coating thickness, CNC alignment, S_{CNC}, and vol% CNC. For example, in the aligned CNC case (*Fig 6b* and *6d*)

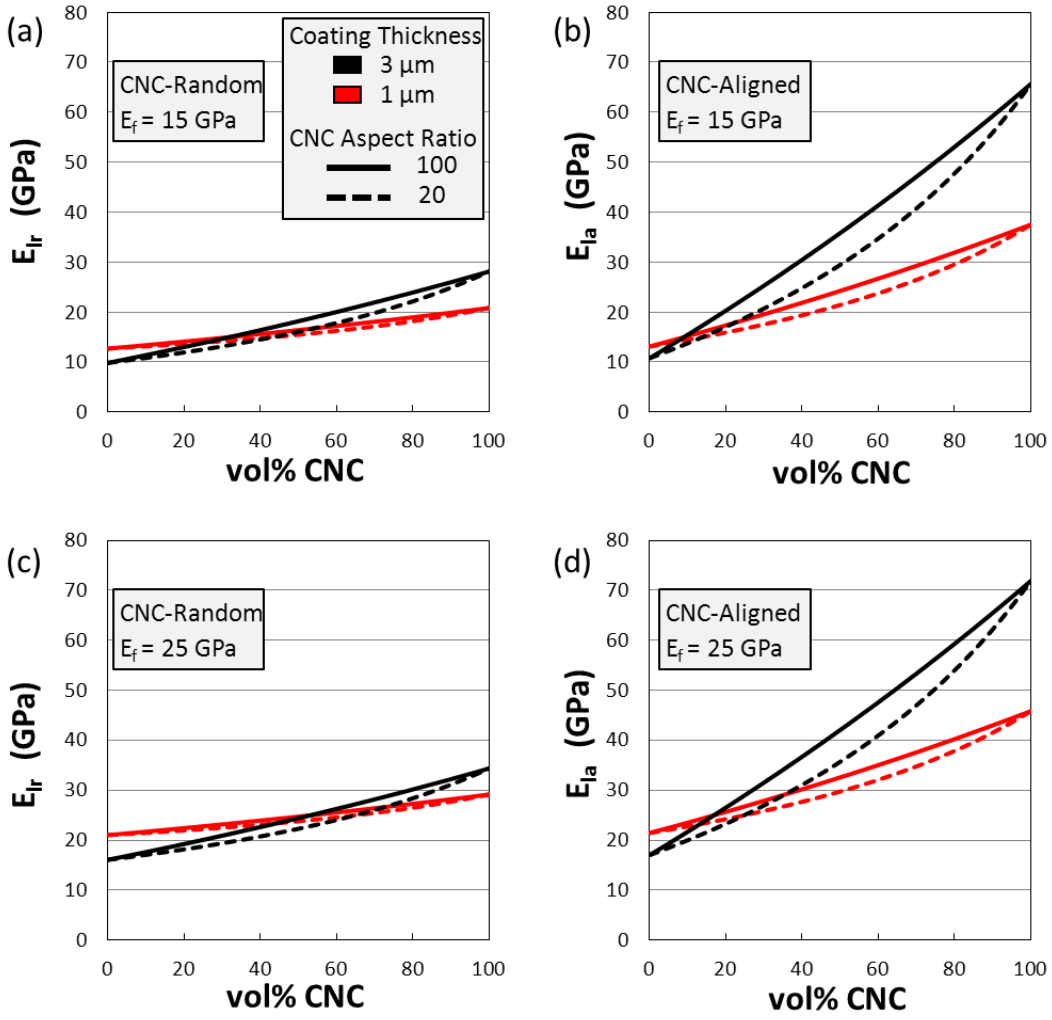

Fig 6 - Laminate theory calculations of the effective elastic modulus of a fiber element coated on the top and bottom surfaces with a CNC-epoxy layer (1 or 3 µm in thickness). The effect of CNC volume percent, CNC configuration (random and aligned) within the epoxy matrix, CNC aspect ratio and the starting fiber elastic modulus, E_f, on the effective elastic modulus of laminate, E_{lx}, has been calculated for, a) random CNC orientation with E_f = 15 GPa, b) aligned CNC orientation with E_f = 15 GPa, c) random CNC orientation with E_f = 25 GPa, d) aligned CNC orientation with E_f = 25 GPa.

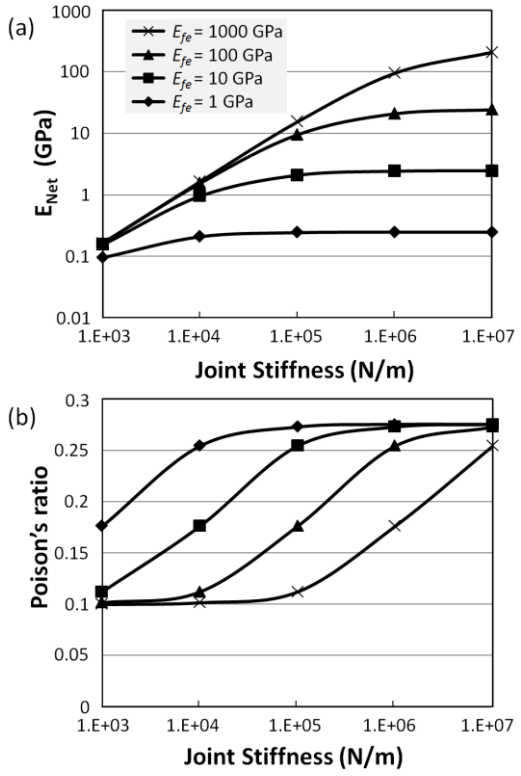

Fig 7 - Network model parametric study showing the role of joint stiffness (k) and fiber element modulus (E_{fe}) on the network structure, a) elastic modulus, E_{net}, and b) Poisson's ratio, ν_{net}. Calculations completed for a network of ρ_{net} = 0.78 g/cm^3, L_f =180 µm, and W_f =30 µm.

whereas for the random CNC case (*Fig 6a* and *6c*), the cross-over point for E_f =15 and 25 GPa fibers occurs at 35 vol% CNC and 55 vol% CNC, respectively. For comparison with experiments, only one study was found in which CNMs were coated on natural fibers. The study by Pommet et al. (2008) deposited bacterial cellulose (BC) onto the surface of sisal and hemp fibers, however, the potential reinforcement potential of the BC coating was masked by an artifact of the BC coating process. Unfortunately, the BC coating process required that the fibers be exposed to the culturing conditions necessary for the bacteria to produce the cellulose, which chemically modified the starting sisal and hemp fibers, and resulted in a reduction in the elastic modulus of the BC coated natural fiber.

Role of fiber element and spring constant on network properties

Modification of the network elastic properties (stiffness and Poisson's ratio) from the addition of CNC-epoxy coating of fiber elements was considered to occur through the enhancement of elastic properties of the fiber element, E_{fe} and the fiber-fiber joint stiffness, k. To assess the relative contributions of changes in E_{fe} and k to the network stiffness, E_{net}, a parametric study over the range of E_{fe} = 1-1000 GPa and k = 1x10^3-1x10^7 N/m was completed (*Fig 7*). The wide design space of E_{fe} and k was used to assess the upper bounds and to clarify realistic bounds for reinforcement from CNCs. While k has not been measured, the parametric study also gives insight into the interplay between E_{fe} and k in affecting E_{net}, making it possible to identify what combinations of fiber reinforcement and joint reinforcement would be most effective for network reinforcement.

The results for E_{net} and ν_{net} as a function of E_{fe} and k are presented in *Fig 7*. In general, increases in E_{fe} result in an increase in E_{net} and a decrease in ν_{net}, while increases in k result in increases for both E_{net} and ν_{net}. There are deviations to these general trends at locations where E_{net} and ν_{net} have plateaued. Regardless of E_{fe} it appears that the ν_{net} varies between 0.1 (at low k) and 0.27 (at high k) thus establishing the bounds for a joint with low and high stiffness, respectively, relative to the fiber element. There is also interplay between E_{fe} and k in affecting E_{net} and ν_{net}. At low E_{fe} (1 GPa), increases in k have a smaller influence on increasing E_{net} and larger influence on increasing ν_{net} as compared to high E_{fe} (1000 GPa). At low k, increases in E_{fe} result in small increases to E_{net}, this area of parameter space is dominated by k. In contrast, at high k, increases in E_{fe} result in large increases to E_{net}, this area of parameter space is dominated by E_{net}. This parametric study showed that E_{net} can be increased with increasing E_{fe}, k, the degree of which is dependent on the interplay between E_{fe} and k. The effect of CNC-epoxy additions on the predicted E_{net} is discussed in the following sub-section.

CNC-epoxy stiffening of fiber network structures

The addition of CNC-epoxy to a fiber network structure will likely alter both the fiber element stiffness and the network joint stiffness. However, since k is unknown for this material system, a joint stiffness of k = 1x10^6 N/m was used, and based on the results in *Fig 7*, this would allow for the maximum sensitivity for changes in the fiber element stiffness in altering the network stiffness. For this case then, the stiffening potential of CNC-epoxy additions on network properties (E_{net} and ν_{net}) was considered to occur through the modification of the fiber element elastic modulus, E_{fe}. Of interest is the ability of the CNC-epoxy additions to stiffen the network structure beyond what can be achieved from the uncoated fiber element. When considering only the starting fiber element with E_f = 15 or 25 GPa, the resulting E_{net} is ~3 GPa, and ~5 GPa, respectively, which is similar to that reported for carton stock and boxboard (E = 6-7.5 GPa) with similar density (ρ_{net} = 0.75-0.78 g/cm^3) (Baum 1984). The laminate theory calculations give the estimated elastic properties of the fiber elements coated with CNC-epoxy, which based on the idealized upper bound values, gives a possible range of E_{fe} = 10-70 GPa (see *Fig 6* for the range of either E_{lr} and E_{la}).

To investigate the stiffening potential of CNC-epoxy additions, a starting network model (ρ_{net} = 0.78 g/cm^3, L_f = 180 µm, W_f = 30 µm, E_f = 25 GPa and k = 1x10^6 N/m) was modified with a CNC-epoxy coating (t_c = 3 µm layer thickness and aligned CNC configuration) of each fiber element. This configuration of the CNC-epoxy coating gives an upper bound of the stiffening potential. So within the network model, E_f was replaced with the coated fiber element elastic modulus, E_{fe} which varied based on the predictions of E_{la} (*Fig 6d*).

Note that it is assumed here that the CNC-epoxy additions altered the elastic modulus of the fiber element, with no changes in the fiber element length or width, so the network density stayed constant. In reality, the addition of the CNC-epoxy would widen the fiber elements and fill some of the porosity within the starting fiber element network, both of which would increasing the density of the network composite, resulting in additional stiffening. This latter contribution to stiffening was not considered in this study.

The results are shown in *Fig 8*. With increasing CNC vol% there is an increase in E_{net} but ν_{net}, appears to be minimally affected. For CNC aspect ratio of 100, the network stiffness increases ~20% for an addition of 10 vol% CNC; further, addition of 50 vol% CNC doubles the network stiffness, suggesting that CNC-epoxy additions have a potential for reinforcing network structures. However, this comparison was for the case at 0 vol% CNC additions, thus the fiber elements had a coating of 100 vol% epoxy, which have E_e = 3.8 GPa, effectively *lowering* the stiffness of the fiber element.

To assess the critical vol% CNC additions necessary to enhance the stiffness of a preformed network structure, then it is necessary to consider the reinforcement of CNC-epoxy coating as compared the original network structure without CNC-epoxy additions (i.e. E_{net} = ~5 GPa). From *Fig 8a*, the cross over point occurs at CNC concentrations of ~ 17 and 22 vol% for the CNC aspect ratio of 100 and 20, respectively, and can be considered the critical vol% CNC. Note that this is based on an upper bound assessment of CNC-epoxy properties, and perfect interface between the CNC-epoxy and fiber element, taking these into account, the critical vol% CNC necessary to reinforce a network structure would shift higher.

The maximum reinforcement potential of CNC additions can be estimated, using the highest reinforcement configuration considered in this study, 100vol% CNC, with perfect CNC alignment and a 3 µm coating thickness (see *Fig 5*). Appling a coating like this on fiber elements having E_f = 25 GPa, then from *Fig 7* the estimated network stiffness would be E_{net} = ~11 GPa, which is an increase of ~2 times the unmodified case. However, as noted earlier, the estimated properties of this coating, E_c = 150 GPa, is an unrealistic upper bound, based on many assumptions. To approximate a more "realistic" upper bound, one should consider that one of the highest reported stiffness for wood based CNC films (100 vol% CNC, highly aligned) was 30 GPa, (Reising et al. 2012), which is 5 times lower than the ~150 GPa. Using E_c = 30 GPa for the coating and interpolating the results of *Fig 5*, *6b*, and *6d* (for the case of 3 µm thick coating of fully aligned CNCs), it is possible to obtain an estimated E_{fe} of ~20 GPa and ~27 GPa for initial fiber elements stiffness of 15 GPa, and 25 GPa, respectively. By using E_{fe} = 20 and 27 GPa, the corresponding elastic modulus of the network would be E_{net} = ~4 GPa and ~5 GPa, respectively, both of which are similar to the stiffness of the initial network without the CNC additions. Note that this can still be considered an upper bound estimate of the CNC reinforcement potential, in that there is no slippage at the CNC coating-fiber element interface and the CNC coating is a significant volume fraction of the coated-fiber system (i.e. two 3 µm thick layers of CNCs, one on either side of a fiber element that is 10 µm thick). Considering this, the stiffening potential of CNC additions on network properties via a mechanism of enhancing fiber element stiffness, appears limited for the case of fiber elements having relatively high stiffness (15-25 GPa).

The implications of these results suggest that for additions of CNCs to a preformed network structure consisting of micron sized fiber elements, such as paper, that the mechanism of enhancing the fiber element properties by the CNC additions will have a limited effect on stiffening the network. However, for fiber elements with lower stiffness, perhaps ~ 1 GPa or lower, the CNC coatings have greater reinforcing potential, which would subsequently stiffen the network structure. Moreover, in real systems, the CNC additions may likely initiate other stiffening mechanisms to the network, such as, altering the fiber-fiber joint stiffness and increase density of the network by filling in voids, effectively increasing the volume fraction of load bearing material, etc. These latter mechanisms were not considered in this study.

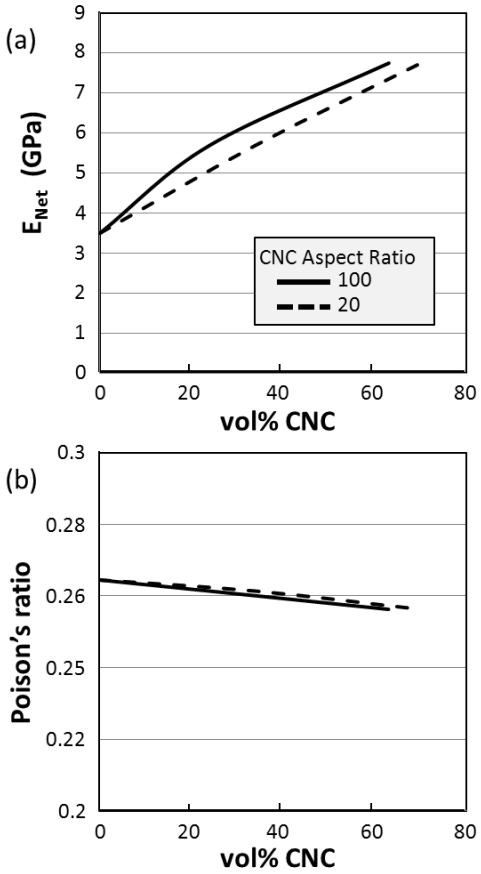

Fig 8 - Network model estimates of a) network modulus, b) network Poisson's ratio, as a function of CNC volume percent, and CNC aspect ratio (20 vs 100). Calculations were based on a fiber element with an initial E_f = 25 GPa that is modified with a 3 µm layer of CNC-epoxy (aligned CNC configuration) with a network characteristics of ρ_{net} = 0.78 g/cm^3, and k = 1x10^6 N/m.

Conclusions

A hierarchal length scale model approach was used for estimating the reinforcement potential of cellulose nanocrystals (CNC) to enhance the properties of fiber network structures. An idealized 2-dimensional (2-D) fiber network structure was subsequently reinforced via CNC-epoxy coating of the individual fiber elements making up the network structure. The reinforcement mechanism on the network structure was considered to occur through the reinforcement of the fiber elements via the CNC-epoxy coating. Micromechanical and laminate theory models demonstrated that reinforcement of the fiber elements via CNC-epoxy coating was dependent on several factors: stiffness of the starting fiber element, CNC-epoxy layer thickness, CNC alignment, and CNC aspect ratio. Fiber elements with greater elastic modulus required increased CNC-epoxy coating thicknesses, greater CNC alignment, greater CNC aspect ratio, and/or greater CNC volume fraction for reinforcement. In the idealized case considered in this study the 2-D network model demonstrated that the reinforcement of fiber elements by CNC-epoxy coatings could enhance the elastic properties of the network structure. Taking into consideration experimentally-obtained property values for CNC films and fiber element properties typical of fibers used in paper products, suggests that the extent to which CNC additions can enhance fiber element stiffness and thus the network stiffness may be limited.

Acknowledgements

The authors are grateful to financial support for this research provided by the Forest Products Laboratory under USDA Grant:07-CR-11111120-093, and 09-JV-11111137-151.

Literature

Araki, J., Wada, M., Kuga, S., and Okano, T. (1998): Flow properties of microcrystalline cellulose suspension prepared by acid treatment of native cellulose, Colloids and Surfaces a-Physicochemical and Engineering Aspects, 142(1), 75-82.

Astrom, J., Saarinen, S., Niskanen, K., Kurkijarvi, J. (1994): Microscopic mechanics of fiber networks, Journal of Applied Physics, 75(5), 2383-2392.

Aulin, C., Gallstedt, M., and Lindstrom, T. (2010): Oxygen and oil barrier properties of microfibrillated cellulose films and coatings, Cellulose, 17(3), 559-574.

Bai, W., Holbery, J., and Li, K.C. (2009): A technique for production of nanocrystalline cellulose with a narrow size distribution, Cellulose, 16(3), 455-465.

Baum, G. (1984): The Elastic Properties of Paper: A Review, The Institute of Paper Chemistry, pp. 1-21.

Beck-Candanedo, S., Roman, M., and Gray, D.G. (2005): Effect of reaction conditions on the properties and behavior of wood cellulose nanocrystal suspensions, Biomacromolecules, 6(2), 1048-1054.

Bondeson, D., Mathew, A., and Oksman, K. (2006) Optimization of the isolation of nanocrystals from microcrystalline cellulose by acid hydrolysis, Cellulose, 13(2), 171-180.

Bronkhorst, C.A. (2003): Modelling paper as a two-dimensional elastic-plastic stochastic network, International Journal of Solids and Structures, 40(20), 5441-5454.

Dri, F.L., Hector, L.G., Moon, R.J., and Zavattieri, P.D. (2013): Anisotropy of the elastic properties of crystalline cellulose I_β from first principles density functional theory with Van der Waals interactions, Cellulose, 20(6), 2703-2718.

Eichhorn, S.J. (2011): Cellulose nanowhiskers: promising materials for advanced applications, Soft Matter, 7(2), 303-315.

Habibi, Y., Lucia, L.A., and Rojas, O.J. (2010): Cellulose Nanocrystals: Chemistry, Self-Assembly, and Applications, Chemical Reviews, 110(6), 3479-3500.

Halpin, J.C., Jerina, K., and Whitney, J.M. (1971): The laminate analogy for 2 and 3 dimensional composite materials, Journal of Composite Materials, 5(1), 36-49.

Halpin, J.C., and Kardos, J.L. (1976): Halpin-tsai equations – review, Polymer Engineering and Science, 16(5), 344-352.

Halpin, J.C., and Pagano, N.J. (1969): The laminate approximation for randomly oriented fibrous composites, Journal of Composite Materials, 3(4), 720-724.

Hassan, E.A., Hassan, M.L., and Oksman, K. (2011): Improving bagasse pulp paper sheet properties with microfibrillated cellulose isolated from xylanase-treated bagasse, Wood and Fiber Science, 43(1), 76-82.

Huang, X.X., Wen, X.F., Cheng, J., and Yang, Z.R. (2012) Sticky superhydrophobic filter paper developed by dip-coating of fluorinated waterborne epoxy emulsion, Applied Surface Science, 258(22), 8739-8746.

Iwamoto, S., Kai, W.H., Isogai, A., and Iwata, T. (2009): Elastic Modulus of Single Cellulose Microfibrils from Tunicate Measured by Atomic Force Microscopy. Biomacromolecules, 10(9), 2571-2576.

Joseleau, J.P., Chevalier-Billosta, V., and Ruel, K. (2012): Interaction between microfibrillar cellulose fines and fibers: influence on pulp qualities and paper sheet properties, Cellulose, 19(3), 769-777.

Juntaro, J., Pommet, M., Kalinka, G., Mantalaris, A., Shaffer, M.S.P., and Bismarck, A. (2008): Creating hierarchical structures in renewable composites by attaching bacterial cellulose onto sisal fibers, Advanced Materials, 20(16), 3122-3126.

Lavoine, N., Desloges, I., Dufresne, A., and Bras, J. (2012): Microfibrillated cellulose - Its barrier properties and applications in cellulosic materials: A review, Carbohydrate Polymers, 90(2), 735-764.

Liu, J.X., Chen, Z.T., and Li, K.C. (2010): A 2-D lattice model for simulating the failure of paper, Theoretical and Applied Fracture Mechanics, 54(1), 1-10.

Ma, H.Y., Burger, C., Hsiao, B.S., and Chu, B. (2011): Ultrafine Polysaccharide Nanofibrous Membranes for Water Purification, Biomacromolecules, 12(4), 970-976.

Moon, R.J., Martini, A., Nairn, J., Simonsen, J., and Youngblood, J. (2011): Cellulose nanomaterials review: structure, properties and nanocomposites, Chemical Society Reviews, 40(7), 3941-3994.

Mott, L., Groom, L., and Shaler, S. (2002): Mechanical properties of individual southern pine fibers. Part II. Comparison of earlywood and latewood fibers with respect to tree height and juvenility, Wood and Fiber Science, 34(2), 221-237.

Pommet, M., Juntaro, J., Heng, J.Y.Y., Mantalaris, A., Lee, A.F., Wilson, K., Kalinka, G., Shaffer, M.S.P., and Bismarck, A. (2008): Surface modification of natural fibers using bacteria: Depositing bacterial cellulose onto natural fibers to create hierarchical fiber reinforced nanocomposites, Biomacromolecules, 9(6), 1643-1651.

Reising, A.B., Moon, R.J., and Youngblood, J.P. (2012): Effect of particle alignment on mechanical properties of neat cellulose nanocrystal films, J-for-Journal of Science & Technology for Forest Products and Processes, 2(6), 32-41.

Rusli, R., and Eichhorn, S.J. (2008): Determination of the stiffness of cellulose nanowhiskers and the fiber-matrix interface in a nanocomposite using Raman spectroscopy, Applied Physics Letters, 93(3), 033111.

Samir, M.A.S.A., Alloin, F., and Dufresne, A. (2005): Review of recent research into cellulosic whiskers, their properties and their application in nanocomposite field, Biomacromolecules, 6(2), 612-626.

Sehaqui, H., Zhou, Q., and Berglund, L.A. (2013): Nanofibrillated cellulose for enhancement of strength in high-density paper structures, Nordic Pulp & Paper Research Journal, 28(2), 182-189.

Silberstein, M.N., Pai, C.L., Rutledge, G.C., and Boyce, M.C. (2012): Elastic-plastic behavior of non-woven fibrous mats, Journal of the Mechanics and Physics of Solids, 60(2), 295-318.

Siro, I., and Plackett, D. (2010): Microfibrillated cellulose and new nanocomposite materials: a review, Cellulose, 17(3), 459-494.

Sturcova, A., Davies, G.R., and Eichhorn, S.J. (2005): Elastic modulus and stress-transfer properties of tunicate cellulose whiskers, Biomacromolecules, 6(2), 1055-1061.

Syverud, K., and Stenius, P. (2009): Strength and barrier properties of MFC films, Cellulose, 16(1), 75-85.

Tang, L.M., and Weder, C. (2010): Cellulose Whisker/Epoxy Resin Nanocomposites, Acs Applied Materials & Interfaces, 2(4), 1073-1080.

Timoshenko, S., and Goodier, J.N. (1951): Theory of Elasticity, 2nd ed. McGraw-Hill Book Company, Inc., New York.

Wu, X.F., and Dzenis, Y.A. (2005): Elasticity of planar fiber networks, Journal of Applied Physics, 98(6), 093501-093501.

Xu, S.H., Girouard, N., Schueneman, G., Shofner, M.L., and Meredith, J.C. (2013): Mechanical and thermal properties of waterborne epoxy composites containing cellulose nanocrystals. Polymer, 54(24), 6589-6598.

Manuscript received November 15, 2013
Accepted January 18, 2014